



Fermi National Accelerator Laboratory

FERMILAB-Conf-91/138-E

Jet Results from CDF*

The CDF Collaboration
Fermi National Accelerator Laboratory
P.O. Box 500
Batavia, Illinois 60510

Presented by
Naor Wainer
(Representing the CDF Collaboration)

May 1991

* Published Proceedings *XXVth Rencontres de Moriond*, Les Arcs, Savoie, France, March 17-24, 1991.



Jet Results from CDF

Naor Wainer
Fermilab
(Representing the CDF Collaboration)

Abstract

Recent results from CDF in jet physics are presented. Tests of leading order and next to leading order QCD are performed by measuring the dijet invariant mass spectrum, jet shapes and three jet events. Tests the leading logarithm approximation in QCD are made by comparing the highest energy events at CDF with the Herwig Monte Carlo.

Published Proceedings XXVth Rencontres de Moriond, Les Arcs, Savoie, France, March 17-24, 1991.

Introduction

CDF has collected approximately 4.5 pb^{-1} of integrated luminosity at $\sqrt{s} = 1800 \text{ GeV}$ of $p\bar{p}$ collisions. This high statistics sample allows more accurate tests of QCD. Fortunately, significant theoretical progress is being made in parallel, either through calculating hard scattering at Next to Leading Order (NLO), or by modeling higher order contributions in the Leading Log Approximation through shower Monte Carlos.

In this paper comparisons of data and QCD calculations are done in three different levels:

1. Tests of Leading Order (LO) QCD. When a higher order calculation is not available, the data was compared with LO QCD. This allows us to understand which features of the data are not well described by theory, and need higher order calculations. In this note the differential cross section $d\sigma/dM_{JJ}$ is measured where M_{JJ} is the invariant mass of a 2 jet system. Also 3-jet distributions are compared with α_s^3 tree level calculations.
2. Tests of Next to Leading Order QCD. In this note we describe a measurement of Jet Shape, a process which is not existent in LO calculations and is obtained when calculating in NLO $d\sigma/dE_t$.
3. Tests of the Leading Log approximation as implemented by the Monte Carlo program Herwig[1]. A comparison is performed between this Monte Carlo and the most energetic events in CDF (measured by the total transverse energy in the calorimeter).

Data Selection

The CDF detector has been described in detail elsewhere [2]. For these measurements, jets in the central, wall and plug calorimeter were used(See fig. 1). For the jet shapes measurement three dimensional tracks in the central tracking chamber were used.

For the dijet analysis, online triggers in which a single jet is required to have transverse energy in the calorimeter above specific threshold were used. The minimum energy required were 20, 40 and 60 GeV. The 20 and 40 GeV triggers were prescaled, in order to maintain a manageable trigger rate.

The jet shape analysis was done using only the jet trigger data which required 60 GeV or more transverse energy. The jets were required to be in the central calorimeter.

The 3-jet analysis and the comparison of high energy events with Herwig were performed with data from a total transverse energy trigger. The trigger required the total transverse energy in the calorimeter to be greater than 120 GeV.

Jet Algorithm

In order to compare theory with data a common jet definition has to be adopted both by experimentalists and theoreticians. A serious attempt to reach a standard is the Snowmass accord [3], in which a common definition was specified. One of the main outcomes is that a jet should be defined by its transverse energy (E_t) and cone size (R).

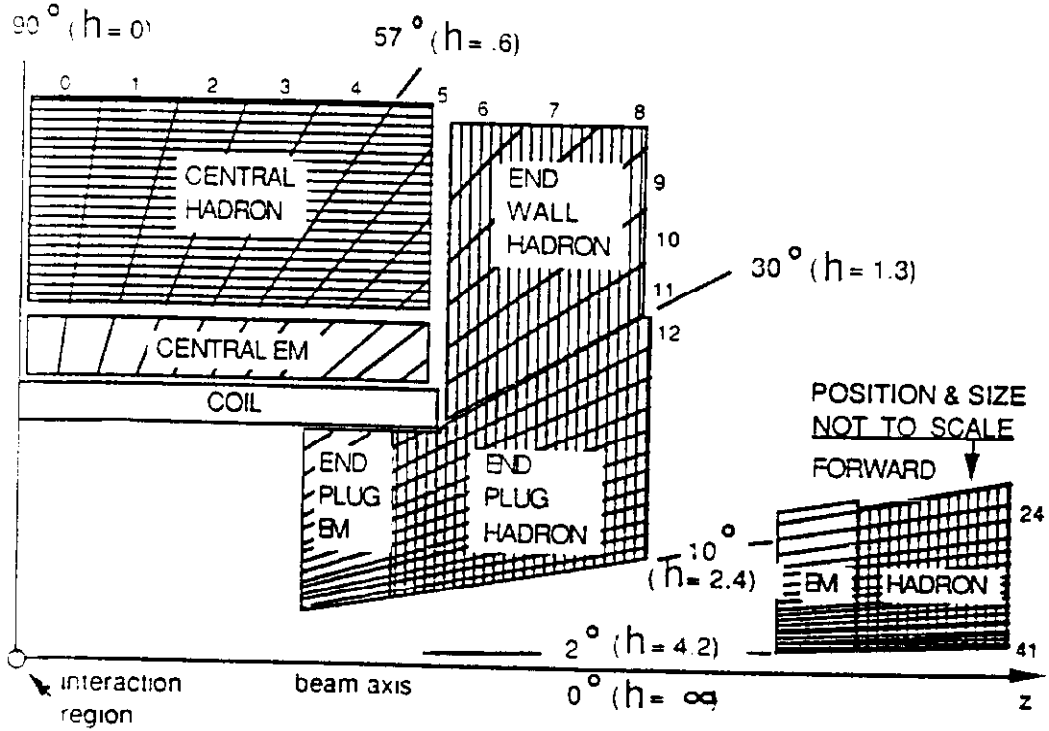


Figure 1: The CDF Calorimeter.

The cone size R is defined as $R = \sqrt{\Delta\eta^2 + \Delta\phi^2}$ where $\eta = \log \cot(\theta/2)$, ϕ is the azimuthal angle difference and θ is the polar angle difference between a tower/particle/parton and the jet axis. One then defines:

$$E_t^{jet} = \sum_{R_i \leq R_0} E_{ti} \quad \eta^{jet} = \frac{1}{E_t^{jet}} \sum_{R_i \leq R_0} E_{ti} \eta_i \quad \phi^{jet} = \frac{1}{E_t^{jet}} \sum_{R_i \leq R_0} E_{ti} \phi_i$$

Where, again, the sums can be over partons, particles or towers within R_0 .

Clearly, the chosen cone size of the jet does not affect LO QCD calculations, but it is important for higher order calculations, where more than one parton can be within the cone.

In order to avoid biases, we do not correct for the two processes that change slightly the jet energy in the cone: particles that due to fluctuations or magnetic field effects slipped out of the cone, and underlying event particles, created by soft processes among the debris of the nucleons, that may fall into the cone. Although predictions of the magnitude of the Jet E_t change due to these processes are model dependent, they tend to be small and negligible at high energies and large cone sizes.

Two Jet Invariant Mass

We measured the dijet invariant mass spectrum. In the center of mass system, the two jets are back to back and, after integration over the azimuthal angle ϕ , the cross section is dependent on the dijet invariant mass M_{JJ} and the azimuthal angle θ .

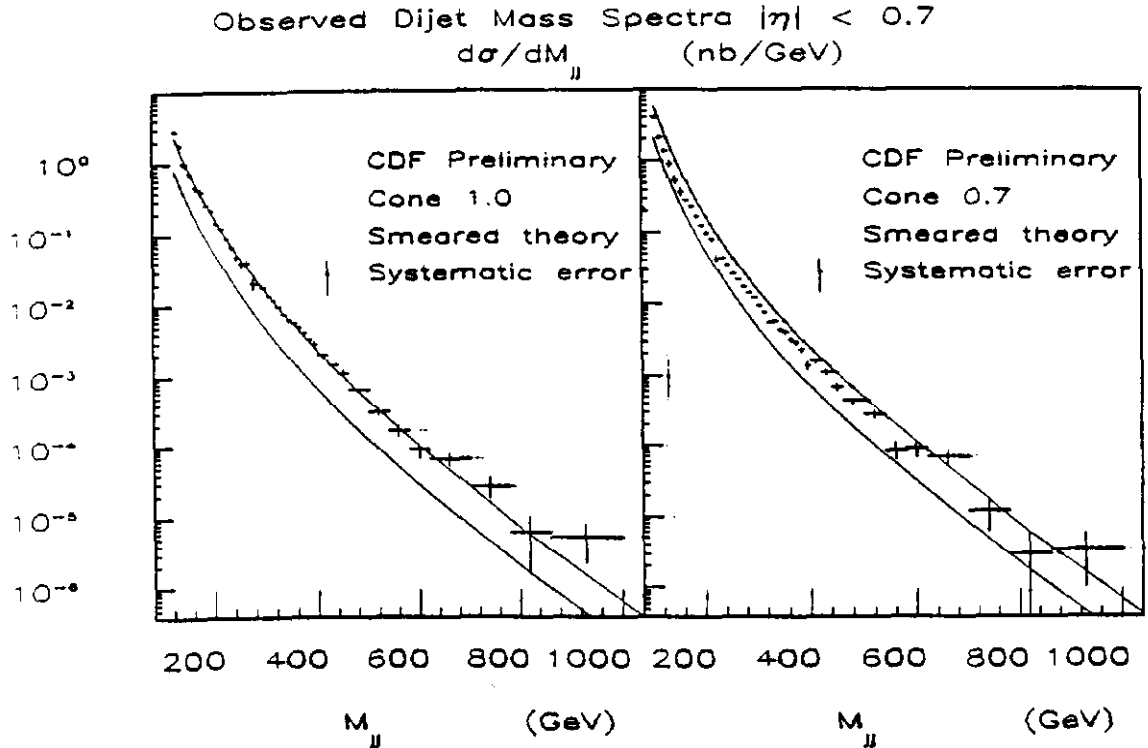


Figure 2: The dijet mass distribution.

As a NLO calculation is not available for M_{JJ} , the data will be compared to the LO QCD calculation. As described above, no out of cone or underlying event correction are applied. The mass is calculated in the usual way $M_{JJ} = \sqrt{(E_1 + E_2)^2 - (\vec{P}_1 + \vec{P}_2)^2}$, where E_j is the energy of jet j , obtained by summing tower energies, and \vec{P}_j is the momentum of the jet, calculated by assigning a vector to each tower and then performing a vector sum within the cone.

Instead of correcting the data for detector response, the theory was smeared, i.e. corrected for the combined effect of the detector response with a rapidly falling M_{JJ} spectrum. The corrections were estimated with the Herwig Monte Carlo and a detector simulation.

In Fig 2 measurements of the cross section $d\sigma/dM_{JJ}$ are shown for 2 different cone sizes, $R = 1$, and $R = 0.7$, integrated in the pseudorapidity range $|\eta| \leq 0.7$. The data are represented by crosses, including systematic errors. The band defined by the two curves represent the theoretical uncertainty, obtained by varying the scale Q^2 within $0.5P_t^2 < Q^2 < 2P_t^2$ and using the following parametrizations of structure functions: EHLQ [4], DO [5], DFLM [6], HMRS [7], and MT [8]. These are absolute scale comparisons.

In order to test the agreement between data and theory on the shape of the distributions, data and theory were normalized. Table 1 shows χ^2 confidence levels for fits using different structure functions, scales and cone sizes. The fitting procedure took into account all system-

Confidence Levels (%)						
$Q^2/P_t^2 =$	1	2	$\frac{1}{2}$	1	2	$\frac{1}{2}$
Structure Functions	Cone 1.0			Cone 0.7		
DFLM101	48	46	47	1	1	< 1
DFLM173	54	52	54	1	1	2
DFLM250	50	52	53	2	2	2
DO1	51	51	47	2	1	< 1
DO2	49	48	48	2	2	2
EHLQ1	40	38	40	< 1	< 1	< 1
EHLQ2	24	21	25	< 1	< 1	< 1
HMRSE	46	48	47	2	1	1
HMRSE	46	46	39	3	4	4
MT155	57	58	54	3	3	2
MT187	56	56	56	2	2	1
MT191	66	65	64	5	6	6
MT212	62	61	59	3	4	3

Table 1: LO QCD vs. M_{JJ} spectrum χ^2 confidence levels in percent.

atic uncertainties. Basically the main difference found is the dependence on the jet cone size. There is not much difference between various structure function parametrizations and energy scales. The cone 1.0 distribution is steeper than the cone 0.7 one. The data with cone of 1.0 agrees well with theory while a cone of 0.7 is disfavored. This effect can occur if higher order diagrams change the energy within the smaller cone size, mainly through bremsstrahlung out of the cone. Another possible effect will be initial state radiation falling within the larger jet cone, increasing its energy. It will be interesting to see if NLO calculations can describe this effect.

Three Jet Events

Another method of testing NLO QCD calculations is to study 3-jet distributions. In this case only tree diagrams were evaluated. The main motivation is the that the calculation shows different angular and energy distributions for the different subprocesses, e.g. $gg \rightarrow ggg$ is more singular than $q\bar{q} \rightarrow ggg$. Based on these distributions, it is interesting to measure the amount of $q\bar{q}$ initiated processes in our 3-jet events sample.

The conventions adopted here are relatively simple: the initial partons are labeled 1 and 2 and the outgoing partons (jets) are labeled 3, 4 and 5, ordered by energy. Two important kinematical angles are defined in the CM frame, namely θ , the angle between jet 3 and the beam axis, and the angle ψ defined as the angle between the plane defined by the 3-jet system (3,4 and 5) and the plane defined by the beam and the hardest jet (1,2 and 3). The scaled energy variables are defined $x_i = 2E_i/M_{3J}$, where M_{3J} is the invariant mass of the 3-jet system.

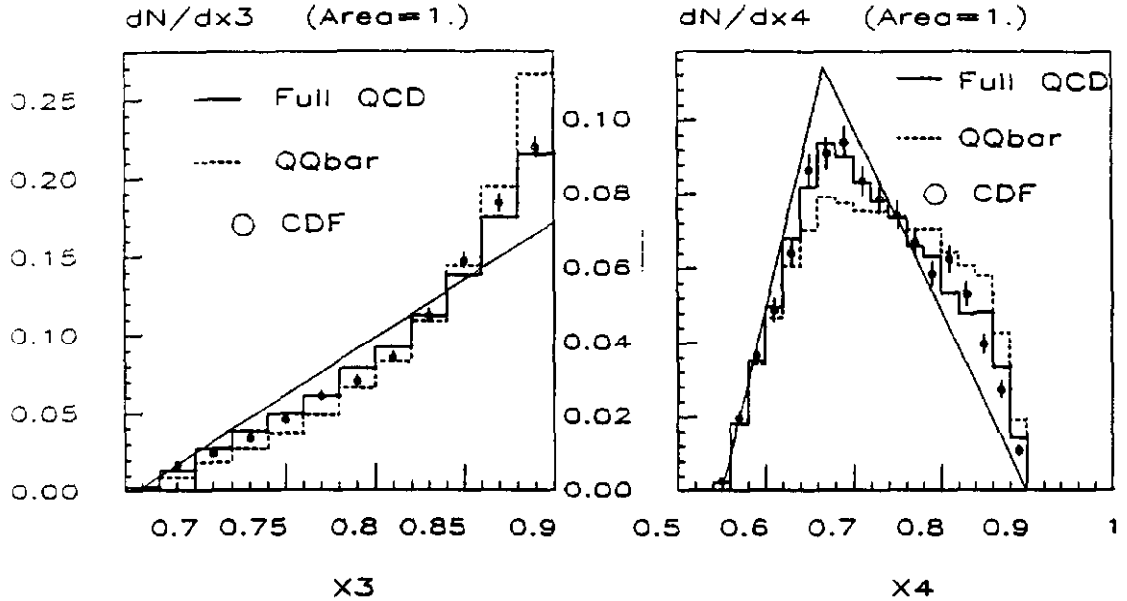


Figure 3: Jet energy fractions in three jet events.

The selection of events reflects the needs of having both well separated jets in the detector and events kinematically away from infrared and collinear divergencies. Events are selected by requiring at least 3 jets with uncorrected $E_t \geq 10$ GeV in the region $|\eta| < 3.5$, separated by $\Delta R \geq 0.85$. Additional cuts avoid trigger biases and divergencies: $M_{3J} > 250$ GeV, $|\cos(\theta)| < 0.6$, $30^\circ < \psi < 150^\circ$ and $x_1 < 0.9$.

The theoretical distributions [10] were obtained by generating 3 partons in the final state away from the infrared or collinear divergencies (cuts similar to those applied on data are applied at parton level) and then fragmenting the partons and processing the event through a detector simulation. Identical cuts as in the data are applied to the generated sample.

The measured cross section is 1.2 ± 0.6 to be compared with the one obtained from theory, 1.8 ± 0.9 . The main uncertainty in the data is energy scale and in the theory is structure functions and renormalization scale used in α_s evaluation.

In Fig. 3 the distributions for x_3 and x_4 are shown. The histograms represent full QCD and a QCD calculation involving only $q\bar{q}$ in the initial state. The linear curves are the phase space predictions. The data clearly prefers the full QCD prediction. The same is observed for the angular distributions, shown in fig. 4. The full QCD distribution is more singular than the $q\bar{q}$ originated distribution, as it shows more prominent peaks when $\cos\theta$ approaches 1, and when ψ approaches 0 or 180 degrees.

The 4 distributions of figs. 3,4 are used to estimate the fraction of $q\bar{q}$ in the initial state. The result of the combined fit is $3_{-3}^{+12}\%$, to be compared to $11 \pm 4\%$, the theoretical prediction.

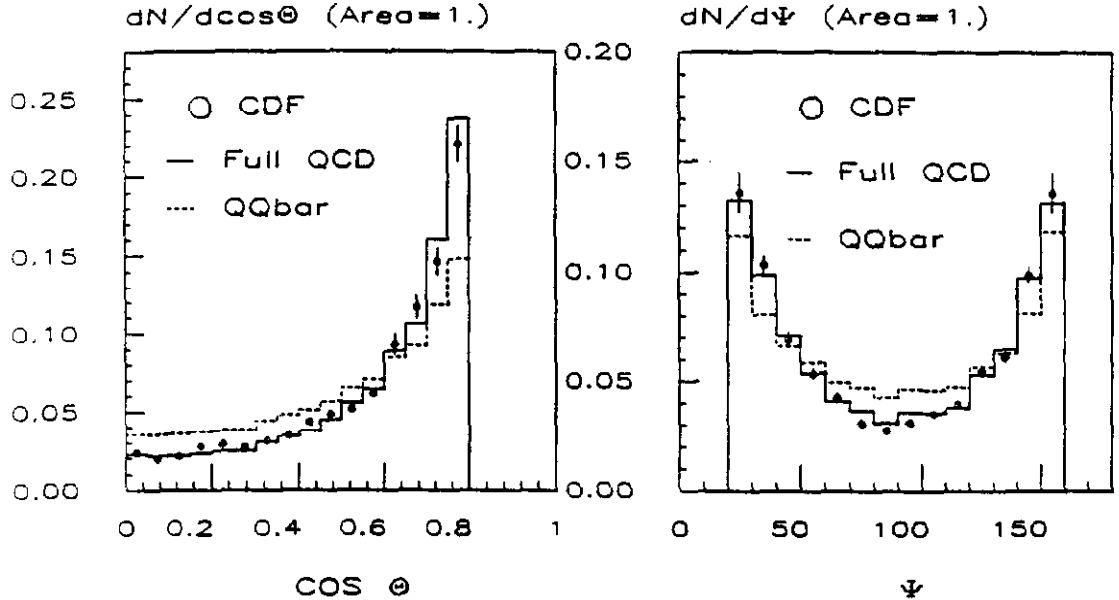


Figure 4: Angular distributions in three jet events.

Jet Shapes

Within the framework of NLO QCD calculations it is possible to obtain more than one parton inside the cone. The jet energy is shared between these two partons. This effect produces an energy distribution inside the jet cone. At high enough energies, where fragmentation effects become negligible, this distribution should be measurable.

To experimentally study the jet shapes, it was decided to use tracks. Tracks have a better spatial resolution than calorimeter towers, which have spatial resolutions on the order of their size. The use of tracks also avoids dealing with calorimeter non-linearities which are large in the P_t range of interest.

To measure the jet shape we define the average P_t density:

$$\rho(r) = \frac{1}{N} \sum_{jets} \frac{1}{P_t^{jet}(R_0)} \sum_{towers} dP_t$$

where dP_t is the the P_t measured in the annular domain between r and $r + dr$. By definition $\int_0^{R_0} \rho(r) dr = 1$, so that P_t^{jet} is also calculated with the tracks. The integral shape variable $\Psi(r) = \int_0^r \rho(r') dr'$ is used to compare data with theory.

In fig. 5 we show both the definition of the variables and the comparison between data and theory. The theory points were calculated for 100 GeV E_t jets. The jets in the data were required to be central, namely $|\eta| \leq 0.7$, and to pass the cut $95 < E_t < 120$ GeV, when the jet E_t was corrected for detector effects. The shape distribution was corrected for tracking

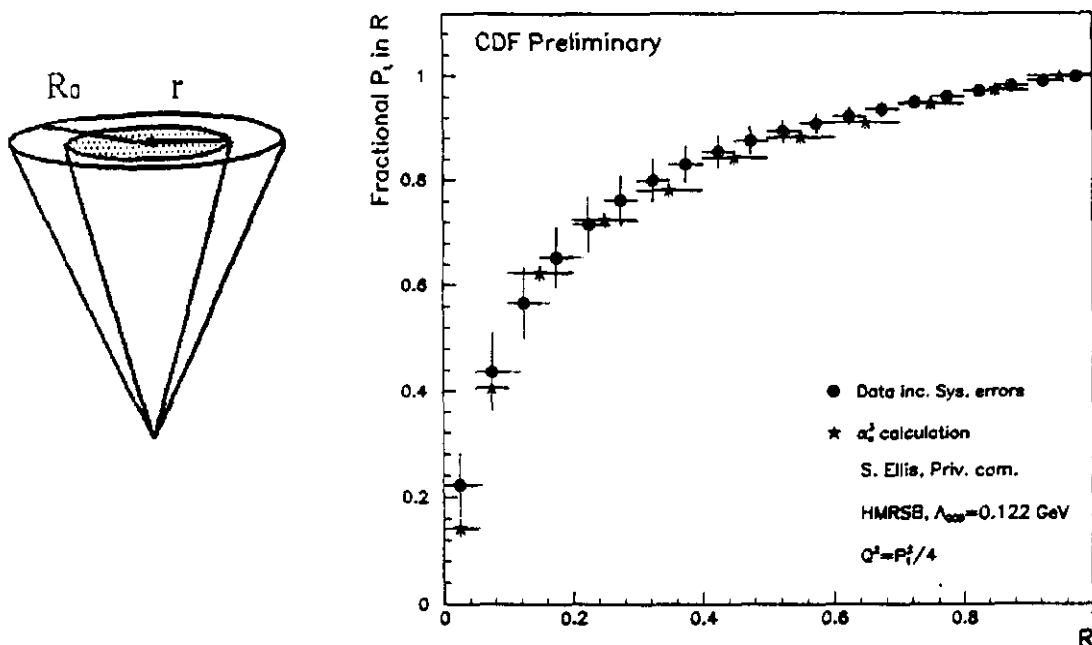
Fractional P_t Flow in 100 GeV Jets, Cone 1.0

Figure 5: Variables and the integral shape of 100 GeV jets.

efficiency effects.

The data show a surprisingly good agreement with theory [9] for a cone $R = 1.0$. The agreement is not as good for other cone sizes (not shown). This effect is under study, as well as the evolution of the shape with jet E_t .

High Total Transverse Energy Events

Events with high total transverse energy ($\sum E_t$) are selected and compared to the parton shower Monte Carlo Herwig version 4.3 with DO1 structure function and $\Lambda_{QCD} = 200$ MeV. The main motivation was to try to detect deviations from QCD in this new energy regime. As a byproduct, this analysis serves as a test of the leading log approximation in this energy regime.

The events were selected by requiring uncorrected $\sum E_t > 400$ GeV, where the sum is over calorimeter towers with $E_t > 500$ MeV. Cosmic rays and events with more than one vertex are rejected.

In Fig 6 the total transverse energy and the missing transverse energy (defined by summing vectorially the E_t of the towers) are shown. The Herwig [1] Monte Carlo describe relatively well the distributions.

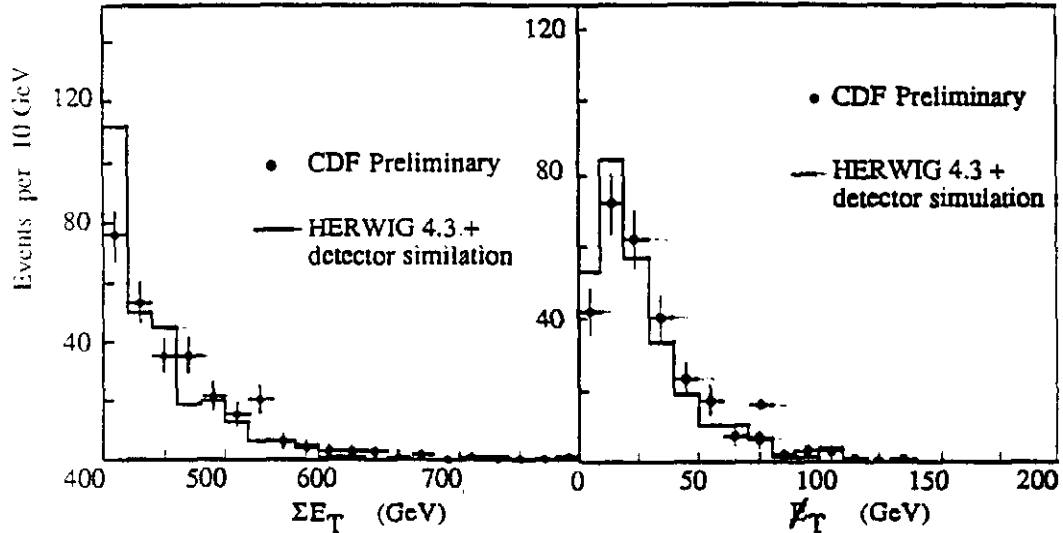


Figure 6: Total and Missing Transverse Energy for the high E_t data sample.

To study how well the Monte Carlo describe the data we study both intra-jet and inter-jet variables. As an example of inter-jet properties of the event, the jet multiplicity, as a function of a jet P_t cut is plotted in fig. 7, for $|\eta| < 2$. The Monte Carlo describe well the data, including the intermediate P_t range (not shown), showing that the leading log approximation describes well the additional creation of soft jets, expected at higher orders.

To probe how well the intra-jet properties are calculate the E_t flow about the Jet axis is calculated. In fig. 7 the E_t flow in ϕ -space is also shown for jets in different P_t ranges. The agreement is very good. The different curves represent different Monte Carlo samples which have the same sizes as the data, and are an estimate of the statistical error in these plots. Similar agreement is found also in η space and for the intermediate P_t range.

Summary

We are probing QCD in all possible levels. A good description of the two jet invariant mass is obtained when one compare and LO QCD calculation with data consisting of cone 1.0 jets. The same cone size is used to compare the shape of 100 GeV jets with a NLO calculations and , again, good agreement is found. Using tree level 3-jet matrix elements we showed that full QCD is needed to describe the data, and estimated the amount of $q\bar{q}$ initiated processes in the data. At the highest energy regime, our events are well described by the Herwig Monte Carlo.

References

- [1] Marchesini and Webber, Nucl. Phys. B310 1988 461.
- [2] Abe et al., CDF Collab., Nucl. Instr. Meth. A271 (1988) 387.

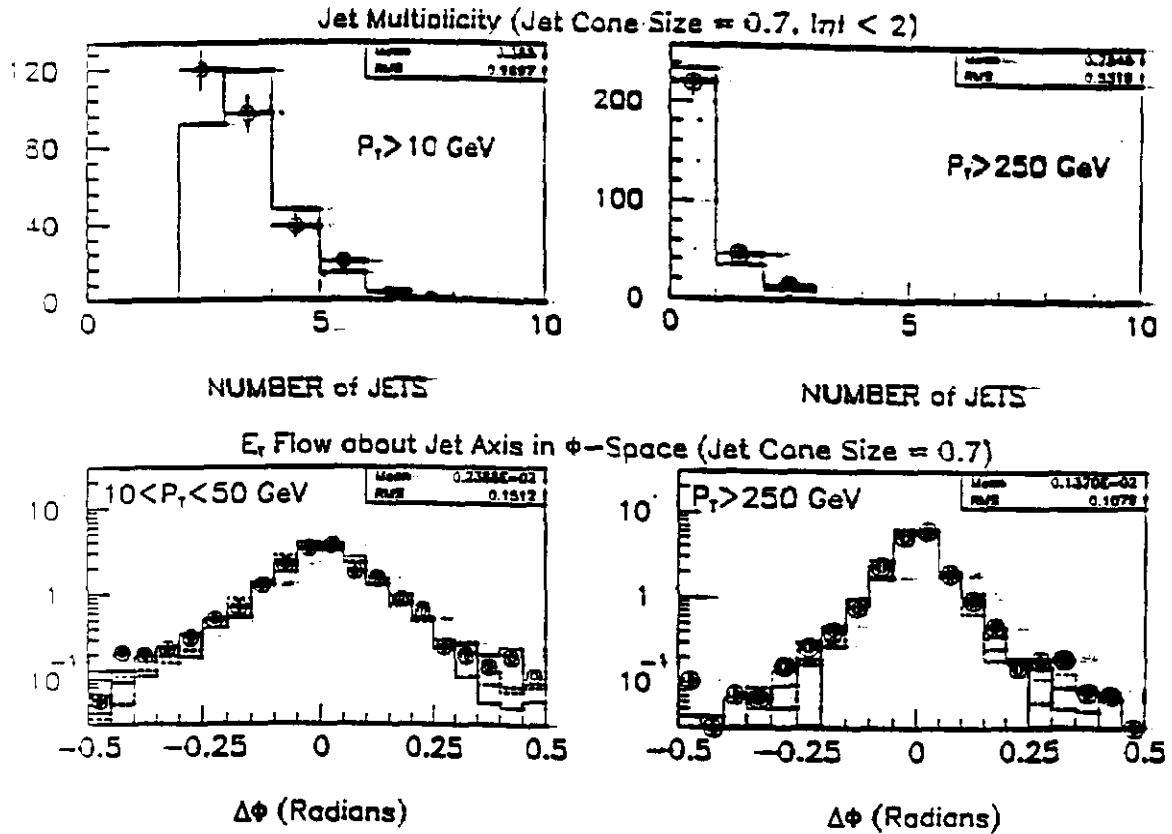


Figure 7: Jet multiplicity and ϕ jet shape in the high E_t data sample for different P_t 's.

- [3] Huth et al., Fermilab-CONF-90/249-E and Proceed. of the Snowmass Summer Study on High Energy Physics (1990).
- [4] Eichten et al., Rev. Mod. Phys. **56** (1984) 579.
- [5] Duke and Owens, Phys. Rev. **D30** (1984) 49.
- [6] Diemoz et al., Z Phys. **C39** (1988) 21.
- [7] Harriman et al., RAL preprint 90-007 (1990).
- [8] Tung and Morfin, Fermilab-PUB-90/74, IIT-PUB-90/11 (1990).
- [9] S.D. Ellis, private communication, based on Ellis, Kunszt and Soper, Phys. Rev. Lett. **64** (1990) 2121.
- [10] Kunszt and Pietarinen, Nucl. Phys. **B164** (1980) 45; Gottschalk and Sivers, Phys. Rev. **D21** (1980) 102; Berends et al., Phys. Lett. **124** (1981) 124.